Perturbation of tunneling processes by mechanical degrees of freedom in mesoscopic junctions

N. F. Schwabe,* A. N. Cleland, M. C. Cross, and M. L. Roukes
Condensed Matter Physics 114-36, California Institute of Technology, Pasadena, California 91125
(Received 26 May 1995)

We investigate the perturbation in the tunneling current caused by nonadiabatic mechanical motion in a mesoscopic tunnel junction. A theory introduced by Caroli *et al.* is used to evaluate second-order self-energy corrections for this nonequilibrium situation lacking translational invariance. Inelastic signatures of the mechanical degrees of freedom are found in the current-voltage $I(V)$ characteristics. These give rise to sharp features in the derivative spectrum, d^2I/dV^2.

I. INTRODUCTION

Electron tunneling has provided valuable insight into the physical properties of solid state systems. Measurement of the current through stationary tunnel junctions has been used to elucidate the density of states in superconductors and many-body properties of metals and semiconductors. Through much theoretical effort, a satisfactory theoretical description of the tunneling process in condensed matter has been attained. Recently, microfabrication techniques have progressed to the point where it is now possible to make extremely compliant vacuum tunneling electrodes which may not remain mechanically stationary during the tunneling process. In the following work we consider the effect that such motion within an elastic tunneling barrier may have upon electron tunneling characteristics. Since, to our knowledge, previous studies of this question have been phenomenological,[1–3] we shall attempt to present a more complete theoretical approach to this problem.

We investigate the characteristics of the tunneling current through a square potential barrier where the barrier is fixed on one side and is allowed to oscillate freely on the other. The goal of this work is thus to predict the effect of a mechanically compliant electrode, which can recoil from a tunneling process, on the current-voltage characteristics and its first and second derivatives. Mathematically this results in the treatment of a localized phonon representing the movable part of the barrier.

In order to treat this problem in a many-body approach which can be extended to more realistic situations than the simplified model considered here, we use a theory treating translationally noninvariant systems under nonequilibrium situations developed in a series of papers by Caroli, Combescot, Nozières, and Saint-James[4–6] (hereafter referred to as CCNS) based on the Keldysh nonequilibrium perturbation formalism.[7] The theory gives a rigorous derivation of an energy-dependent transfer term from first principles, thereby extending the first, more phenomenological approach of Bardeen,[8] and it allows for a treatment of the phonon perturbation in the usual diagrammatic theory.

The principle introduced in Ref. 4 can be used to treat a nonequilibrium situation such as occurs in metal insulator metal (M-I-M) tunneling. It consists of making one or more partitions in the system, allowing for a separate treatment of regions in equilibrium. The separate parts are then joined through an appropriate transfer term. For an arbitrary one-electron potential Caroli *et al.* showed that this method yields an exact treatment. CCNS then derived in Ref. 5 the well-known expression for the tunneling current $I(V)$ through a rigid square barrier for a quasiequilibrium situation. Even though the series of papers starts with a discrete model, CCNS later make a transition to a continuous representation which we use for the calculations in the present paper. They then consider electron-phonon interaction effects in two following papers,[6,9] but the discussion of the effects remained incomplete since a treatment of real phonons is rather involved. The reason is that, for many-body potentials, the evaluation has to be done more carefully, as renormalizations due to many-body effects will always depend on the whole system rather than just pieces of it. However, in special cases such as the one presented here, it can be shown that a simple approximation will work very well.

II. OUTLINE OF THE CALCULATION

Our physical system consists of a mechanically compliant cantilevered metal tip of mass m_c, placed a small distance $2a$ from a stationary bulk metal counterelectrode (see Fig. 1). The movable tip assembly, which we shall refer to as the "cantilever," is modeled as a spring with Hooke's law force constant k_c. Electrical contacts are made to the tip and the counterelectrode. A voltage V is applied across these electrodes and the resulting characteristic of the current I is measured as a function of the applied voltage. In our model Hamiltonian of the system, the metal tip is considered to be a single-mode harmonic oscillator with characteristic frequency ω_c. Assuming a quasiequilibrium situation of equal

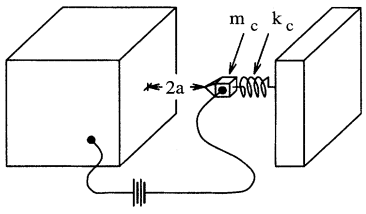

FIG. 1. Schematic view of tunneling electrode on cantilever with mass m_c and spring constant k_c, placed a distance $2a$ from an infinitely massive counterelectrode. The device is biased with a voltage V and the resulting current I is measured.

0163-1829/95/52(17)/12911(10)/$06.00

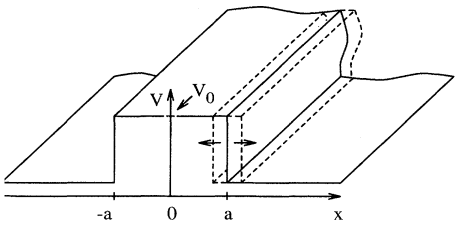

FIG. 2. Full potential barrier used in the calculation. The tunnel barrier has height V_0 and equilibrium width $2a$. The right hand side of the barrier corresponds to the position of the cantilever tip along the x axis.

Fermi energies ($\epsilon_F^r \simeq \epsilon_F^l$) and the simple case of equal work functions for both sides, the resulting potential barrier can be approximated by a square barrier with barrier height V_0. The oscillation of the cantilever simply adds an additional degree of freedom, resulting in a modulation of the barrier width on one side (see Fig. 2). Hence our quantum mechanical Hamiltonian reads

$$H=\frac{\vec{p}_e^{\,2}}{2m_e}+\frac{p_c^2}{2m_c}+\tfrac{1}{2}k_c x_c^2+V_0[\,\theta(x_e+a)-\theta(x_e-x_c-a)\,]\ , \tag{1}$$

where the subscripts e and c refer to the tunneling electron and the cantilever, respectively, while x_c is the instantaneous displacement of the cantilever from its equilibrium position, and p_c is the corresponding momentum. Also θ is the usual unit step function.

To treat the additional term in perturbation theory the potential term is expanded to first order in x_c, which yields $V_r(x_e,x_c)=V_0[\,\theta(x_e+a)-\theta(x_e-a)\,]+x_c V_0\delta(x_e-a)$. In order to apply a many-body treatment to this problem we follow the approach of Ref. 5 and split the system into two halves by adding an infinite potential barrier in the middle of the unperturbed barrier. We thus obtain two subparts similar to the Appendix of Ref. 6 with the potential terms $V_r(x_e,x_c)=V_0\theta(-x_e+a)+x_c V_0\delta(x_e-a)$ for $x>0$ and $V_r(x_e,x_c)=\infty$, for $x<0$ for the right hand side medium and $V_l(x_e,x_c)=V_0\theta(x_e+a)$ for $x<0$ and $V_l(x_e,x_c)=\infty$, for $x>0$ for the left one (see Fig. 3). As in Ref. 6 we shall assume that these two resulting subparts are semi-infinite in the direction perpendicular to the barrier, while at the same

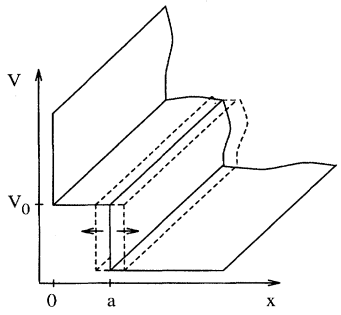

FIG. 3. Semi-infinite potential barrier used to split the Hamiltonian into two pieces. The potential goes to infinity at $x=0$, is equal to V_0 for $0<x<a$, and is zero elsewhere.

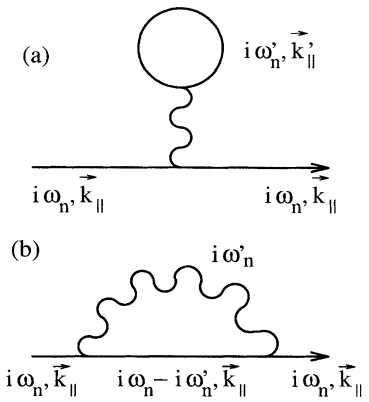

FIG. 4. Lowest-order diagrams contributing to the self-energy: (a) direct and (b) exchange. Electron paths are shown by straight lines and cantilever "phonon" paths are shown by sinuous lines.

time having a finite cross sectional area $\nu^{(2)}$ on which we impose periodic boundary conditions. In second quantized notation the Hamiltonian for the right side reads

$$H_r=\sum_{\vec{q}}\frac{\vec{k}_q^{\,2}}{2m_e}c_{\vec{q}}^{\dagger}c_{\vec{q}}+\omega_c(a^{\dagger}a+\tfrac{1}{2})$$
$$+x_0V_0\sum_{q_x,q_{x'},q_\parallel}c_{q_x,q_\parallel}^{\dagger}c_{q_{x'},q_\parallel}\phi_{q_x}^{*}(a)\phi_{q_{x'}}(a)(a^{\dagger}+a)\ , \tag{2}$$

where the $x_0=\sqrt{1/2m_c\omega_c}$, the root mean square zero point displacement of the cantilever, and we use $\hbar\equiv 1$. Also the variable x labels the coordinate perpendicular to the barrier. In this representation the wave functions ϕ_{q_x} are the x-dependent components of wave functions $\chi_{\vec{q}}$ which diagonalize the system when the unperturbed barrier is included; we will discuss their explicit form later. We will follow the procedure used in Ref. 5 to obtain an expression for the current across the barrier $I(V)$ [see their Eqs. (41), (46), (47)], and for dI/dV, d^2I/dV^2 as well as corrections to these quantities, following the procedure in Ref. 6. As indicated in our model Hamiltonian, we assume that the barrier width does not fluctuate spatially—this leads to perfectly specular transmission. The unperturbed Green's functions for both parts of the system have been calculated in the Appendix of Ref. 6 and will be used as the starting point for further calculations.

Following Ref. 6, to calculate the current we first obtain a self-energy correction for the unperturbed Green's functions of our system, which are then used to determine the corrections for the function γ introduced in Ref. 5, Eqs. (17), (30). (Also see below for definitions.) The first-order terms in the S-matrix expansion for the self-energy vanish, and so we consider the second-order direct and exchange diagrams (see Fig. 4). These terms are dominant due to the heavy mass of the cantilever.[10] A three-dimensional calculation for the Green's function is used to provide a more realistic situation than the one-dimensional model introduced by Caroli *et al.* Due to the translational symmetry in the directions parallel to the barrier, we Fourier transform our Green's functions in

these directions, and we obtain the expressions for $I(V)$ by integrating over the distribution of possible $k_\parallel$ vectors. For the dispersion we assume a single parabolic band and leave the electronic rest mass unaltered for simplicity. We adopt the notation used by CCNS, that is, the following: G, total propagator of the coupled system including phonon corrections; G^0, propagator of the total system without phonon corrections; g, propagator of the right hand side infinite medium including phonon corrections; g^0, propagator of the right hand side infinite medium without phonon corrections; $\tilde{g}$, propagator of the left hand side infinite medium including phonon corrections; $\tilde{g}^0$, propagator of the left hand side infinite medium without phonon corrections; and $\gamma(x_0) \equiv -(1/2m)\lim_{x,x' \to x_0} \partial_x \partial_{x'} g(x,x';k_\parallel;\omega)$ (with $\tilde{\gamma}$ defined accordingly).

The quantity γ is related to the Green's functions of the semi-infinite media, which was introduced in Eq. (17) of Ref. 5; we refer the reader there for a detailed treatment.

The corresponding expressions for g^0 and $\tilde{g}^0$ were derived in the Appendix of Ref. 6. In our case the three-dimensional treatment alters the ω dependence slightly. The resulting differential equation for the semi-infinite medium on the right hand side, after Fourier transformation in the $k_\parallel$ direction, now reads

$$\left[-\frac{1}{2m}\left(\frac{\partial^2}{\partial x^2} - k_\parallel^2 \right) + V_r(x) - (\omega+\mu) \right] g^{0r}(x,x';k_\parallel;\omega) = -\delta(x-x') \ , \tag{3}$$

where the superscript r denotes the retarded function and $V_r(x)$ has the shape shown in Fig. 3.

Explicitly, the unperturbed retarded Green's function g^{0r} is given by

$$g^{0r}(x,x';k_\parallel;\omega) = \begin{cases} -2m\dfrac{\sinh Kx}{KD}[(K+iq)\exp\{K(x'-a)\}+(K-iq)\exp\{K(a-x')\}], & x<x'<a, \\ -2m\dfrac{\sinh Kx'}{KD}[(K+iq)\exp\{K(x-a)\}+(K-iq)\exp\{K(a-x)\}], & x'<x<a, \\ -2m\dfrac{\sinh Kx'}{KD}2K\exp\{iq(x-a)\}, & x>a, \end{cases} \tag{4}$$

where $K=\sqrt{2m[V_0-[\omega+\mu-(k_\parallel^2/2m)]]}$ and $q=\sqrt{2m[\omega+\mu-(k_\parallel^2/2m)]}$ denote the wave vectors inside and outside the barrier, respectively, and the denominator D is given by $D=(K+iq)\exp(-Ka)+(K-iq)\exp(Ka) = 2[K\cosh(Ka)-iq\sinh(Ka)]$. For small barrier transparencies, which are considered here, $\exp(Ka) \gg 1$ and the denominator is then approximately $D=(K-iq)\exp Ka$.

III. SELF-ENERGY CORRECTIONS

A. Dyson equation for the self-energy

Since our system is not translationally invariant, we must resort to a Dyson equation in coordinate representation for the direction perpendicular to the barrier. We make the approximation, which will be justified in the following, that only the electronic subsystem on the right will receive any corrections from coupling to the mechanical degree of freedom. As the calculations for the unperturbed Green's functions on both sides are analogous, we will confine ourselves to calculating g, the propagator of the right subsystem. Ultimately, as shown in Ref. 5, it is necessary to obtain corrections to the Green's functions g^{0+} and g^{0-} occurring in the Keldysh formalism in order to calculate a correction to the current. They are defined in Keldysh[7] and also in Eq. (15) of Ref. 5 as

$$g^{0+}(\omega) = 2\pi i \rho^0(\omega) f^0(\omega) \ , \tag{5}$$

$$g^{0-}(\omega) = 2\pi i \rho^0(\omega)\{f^0(\omega)-1\} \ .$$

Here $\rho^0(\omega)$ and $f^0(\omega)$ are the spectral density and the Fermi occupation function of the right subsystem, respectively. However, in the quasiequilibrium situation considered here, these can be obtained from the renormalized retarded Green's function g^r. The corresponding Dyson equation reads

$$g^r(x,x';k_\parallel;\omega) = g^{0r}(x,x';k_\parallel;\omega) + \int dx''dx''' g^{0r}(x,x'';k_\parallel;\omega)\tilde{\Sigma}^r(x'',x''';k_\parallel;\omega) g^r(x''',x';k_\parallel;\omega) \ . \tag{6}$$

Due to the localization of the electron-cantilever interaction the self-energy has the form

$$\tilde{\Sigma}^r(x'',x''';k_\parallel;\omega) = \delta(x''-a)\,\delta(x'''-a)\Sigma^r(a,a;k_\parallel;\omega) \tag{7}$$

and the integration simplifies to

$$g^r(x,x';k_\parallel;\omega) = g^{0r}(x,x';k_\parallel;\omega) + g^{0r}(x,a;k_\parallel;\omega)\Sigma^r(a,a;k_\parallel;\omega) g^r(a,x';k_\parallel;\omega) \ . \tag{8}$$

Expressed in terms of the unperturbed Green's function this is

$$g^r(x,x';k_\parallel;\omega)=g^{0r}(x,x';k_\parallel;\omega)+\frac{g^{0r}(x,a;k_\parallel;\omega)\Sigma^r(a,a;k_\parallel;\omega)g^{0r}(a,x';k_\parallel;\omega)}{1-g^{0r}(a,a;k_\parallel;\omega)\Sigma^r(a,a;k_\parallel;\omega)}. \tag{9}$$

B. Self-energy in Migdal's approximation

In our system, the cantilever mass m_c is much larger than the electron mass m_e so that Migdal's approximation[10] holds well. The self-energy corrections will be small and the largest contribution to the self-energy will come from the second-order direct and exchange diagrams (see Fig. 4). Higher-order diagrams will only contribute as $\sqrt{m_e/m_c}$, which in our case is certainly small. In view of the fact that we are calculating the lowest relevant orders of the corrections, we also neglect the second term in the denominator of (9). In the Matsubara representation the direct and exchange diagrams are

$$\Sigma^{1d}(a,a;k_\parallel;i\omega_n)=-(x_0V_0)^2D^0(0)\frac{\nu^{(2)}}{\beta}\int\frac{d^2k'_\parallel}{(2\pi)^2}\sum_{i\omega'_n}G^0(a,a;k'_\parallel;i\omega'_n) \tag{10}$$

and

$$\Sigma^{1ex}(a,a;k_\parallel;i\omega_n)=-(x_0V_0)^2\frac{1}{\beta}\sum_{i\omega'_n}D^0(i\omega'_n)G^0(a,a;k_\parallel;i\omega_n-i\omega'_n)\ . \tag{11}$$

In (10) Σ^{1d} does not depend on $k_\parallel$, $\nu^{(2)}$ is the cross sectional area of the junction, and $\beta=(k_BT)^{-1}$. The single-mode phonon propagator is defined as

$$D^0(i\omega_n)=\frac{2\omega_c}{\omega_c^2+\omega_n^2}\ . \tag{12}$$

The fact that there is no integration over the parallel momentum in the exchange term results from the fact that the electron-cantilever interaction is invariant in the transverse direction. The direct term from (10) is not of any further interest, since it just renormalizes the equilibrium position of the cantilever, and we assume that this correction is already included in the definition of the distance $2a$. Due to the symmetry in the problem the wave function $\chi_{\vec{k}}$ of the entire system including the rigid square barrier factorizes as

$$\chi_{\vec{k}}(\vec{r})=\phi_{k_x}(x)\zeta_{k_\parallel}(\vec{\rho})\ , \tag{13}$$

where ρ labels the coordinates in the parallel directions in real space and $\zeta_{k_\parallel}(\vec{\rho})$ is just a two-dimensional plane wave. We can use this to perform the frequency summation in (11) using the representation for G^0 [cf. Eq. (28) of Ref. 5],

$$G^0(a,a;k_\parallel;i\omega_n)=\sum_{k_x}\frac{\phi^*_{k_x}(a)\phi_{k_x}(a)}{i\omega_n-\varepsilon_{\vec{k}}}\ . \tag{14}$$

One further conceptual difficulty in calculating an exchange interaction diagram is that an electron can, in principle, travel from the position of the cantilever through the barrier to the fixed electrode, and back again. This is why we have to take the propagators of the entire system as indicated in (10) and (11). There is an analogous correction to the left side propagator $\tilde{g}^0$, since an electron could travel to the oscillator position on the right and back again. These processes would allow the full semi-infinite propagators g and $\tilde{g}$ to pick up a dependence on the chemical potential on the left hand side and right hand side, respectively. For the small barrier transparencies considered here, contributions arising from these processes can be shown to be negligible (see also Sec. 3 of Ref. 5). To a very good approximation we can therefore replace G by g in (10) and (11). We also replace in (14), the k-sum representation for g, the full wave functions ψ by the wave functions ϕ, which are the analogous solutions for the semi-infinite problem. These wave functions are given by

$$\phi_{k_x}(x)=\begin{cases}\dfrac{4i\tilde{q}}{\tilde{D}}\sinh(\tilde{K}x)e^{-i\tilde{q}a}, & 0<x<a,\\[2ex] e^{-i\tilde{q}x}-e^{i\tilde{q}(x-2a)}\dfrac{2(\tilde{K}\cosh\tilde{K}a+i\tilde{q}\sinh\tilde{K}a)}{\tilde{D}}, & a<x,\end{cases} \tag{15}$$

where now $\tilde{K}=\sqrt{2mV_0-k_x^2}$, $\tilde{q}=|k_x|$ and $\tilde{D}=2(\tilde{K}\cosh\tilde{K}a-i\tilde{q}\sinh\tilde{K}a)$. The k-sum representation for g is then

$$g^0(a,a;k_\parallel;i\omega_n)=\sum_{k_x}\frac{4k_x^2\sinh^2(\sqrt{2mV_0-k_x^2}a)}{2mV_0-k_x^2+2mV_0\sinh^2(\sqrt{2mV_0-k_x^2}a)}\frac{1}{i\omega_n-\varepsilon_{\vec{k}}}\ . \tag{16}$$

In order to simplify the notation, we omit the dependence of our functions on $k_\parallel$ and a for the moment, and we set

$$f(k_x)=\frac{4k_x^2\sinh^2(\sqrt{2mV_0-k_x^2}a)}{2mV_0-k_x^2+2mV_0\sinh^2(\sqrt{2mV_0-k_x^2}a)} . \tag{17}$$

The Matsubara summation in (11) is standard and yields

$$\Sigma^{1\mathrm{ex}}(i\omega_n)=-(x_0V_0)^2\sum_{k_x} f(k_x)\left[\frac{n_B(\omega_c)+n_F(\varepsilon_{\vec{k}})}{i\omega_n+\omega_c-\varepsilon_{\vec{k}}}+\frac{n_B(\omega_c)+1-n_F(\varepsilon_{\vec{k}})}{i\omega_n-\omega_c-\varepsilon_{\vec{k}}}\right] , \tag{18}$$

where $\varepsilon_{\vec{k}}=\dfrac{k^2}{2m}-\mu$ and n_F and n_B are the Fermi and Bose distribution functions:

$$n_F(\varepsilon)=\frac{1}{e^{\beta\varepsilon}+1} \quad \text{and} \quad n_B(\omega)=\frac{1}{e^{\beta\omega}-1} .$$

If (18) is considered at zero temperature, the Fermi distribution functions turn into θ functions and the Bose contributions vanish, so that

$$\Sigma^{1\mathrm{ex}}(i\omega_n)=-(x_0V_0)^2\sum_{k_x} f(k_x)\left[\frac{\theta(-\varepsilon_{\vec{k}})}{i\omega_n-\varepsilon_{\vec{k}}+\omega_c}+\frac{\theta(\varepsilon_{\vec{k}})}{i\omega_n-\varepsilon_{\vec{k}}-\omega_c}\right] . \tag{19}$$

As it turns out, the zero temperature approximation is not very accurate for realistic parameters of a model system. The effects of residual temperature will be considered more thoroughly in Sec. IV B and the Appendix.

The result of (19) can be analytically continued ($i\omega_n\rightarrow\omega+i\delta$) to yield the retarded function.

It should be remarked at this point that within the full Keldysh formalism for fully nonequilibrium situations, the Dyson equation (9) in its correct form would read

$$g^+=(1+g^r\Sigma^r)g^{0+}(1+g^a\Sigma^a)+g^r\Sigma^+g^a , \tag{20}$$

where the superscripts r and a refer to the advanced and retarded functions, respectively [cf. Eq. (5a) in Ref. 6]. Also the retarded self-energy would not just be a convolution of G^r and D^r, but [cf. Eq. (6) in Ref. 6]

$$\Sigma^r\propto(D^r*G^-)+(D^+*G^r). \tag{21}$$

However, in our quasiequilibrium case both equations return to their usual equilibrium form. The main point in which the CCNS formalism enters our treatment is that we will renormalize the quantity γ defined above to obtain a correction for the current in the next section. It is well known that the tunneling current across the unperturbed barrier is a nonlinear function of the applied bias V for large enough biases, although the expression can be linearized for small biases. The modulation of the barrier width introduces a second, small energy scale, so that the resulting contribution to the differential conductivity significantly depends on V even for small values of the bias.

Following an approach by Rickayzen[11] and Scalapino[12] the k sum is assumed to have its strongest contributions coming from the immediate vicinity of the Fermi surface. Going over to an integral representation of the sum and changing the sign of $\varepsilon_{\vec{k}}$ in the first term of (19), we find

$$\Sigma_r^{1\mathrm{ex}}(\omega)=-(x_0V_0)^2N^{1D}(0)f(\sqrt{2m\mu-k_\parallel^2})\int_0^\infty\left[\frac{1}{\omega+\omega_c+\varepsilon+i\delta}+\frac{1}{\omega-\omega_c-\varepsilon+i\delta}\right]d\varepsilon , \tag{22}$$

where $N^{1D}(0)=\sqrt{2m}/2\pi(\sqrt{\mu-(k_\parallel^2/2m)})^{-1}$ is the one-dimensional density of states at the Fermi surface including the sum over two spin directions.

At this point it would be natural to attempt to include the effects of finite mechanical damping in the cantilever motion. However, it is difficult to include such effects from first principles and beyond the scope of this first approach prescribed herein. Instead, a simple way to model the effects of damping is to change ω_c to the frequency for a damped classical harmonic oscillator, satisfying the equation of motion

$$\ddot{x}+\frac{\omega_c}{Q}\dot{x}+\omega_c^2x=0 , \tag{23}$$

which has the solutions $\omega=i\omega_c/2Q\pm\omega_c\sqrt{1-(1/4Q^2)}$. This replacement just introduces a finite imaginary part into the Green's function to achieve line broadening and finite peak heights related to the Q of a classical oscillator. For simplicity let $b\equiv\omega_c\sqrt{1-(1/4Q^2)}$ and $c\equiv\omega_c/2Q$. The self-energy can then be written

$$\Sigma_r^{1ex}(\omega)=(x_0V_0)^2Nf\Sigma^b(\omega) , \tag{24}$$

where

$$\Sigma^b(\omega)=\int_0^\infty d\varepsilon\left[\frac{(\omega+b+\varepsilon)-ic}{(\omega+b+\varepsilon)^2+c^2}+\frac{(\omega-b-\varepsilon)-ic}{(\omega-b-\varepsilon)^2+c^2}\right]=\tfrac{1}{2}\ln\left|\frac{(\omega-b)^2+c^2}{(\omega+b)^2+c^2}\right|-i\left[\pi-\arctan\left(\frac{b-\omega}{c}\right)-\arctan\left(\frac{b+\omega}{c}\right)\right]. \tag{25}$$

The real part of $\Sigma^b(\omega)$ in (25) has the usual logarithmic form for this kind of diagram and the imaginary part is a smoothed-out version of the θ functions occurring for zero damping.

IV. CORRECTIONS FOR THE CURRENT

A. Derivation of the corrections

The self-energy obtained in the last subsection can now be inserted into the simplified version of (9) to yield a correction for the right hand side propagator g, which is needed to calculate the corrections to the current and its first and second derivatives. We will use the same representation of the current as in Eq. (41) of Ref. 5 with the only changes due to the three-dimensional nature of our model, so that the expression for the total specular current I_x across the barrier is proportional to the cross sectional area of the system. Dropping the subscript, it reads

$$\langle I(V)\rangle=8e\nu^{(2)}\int_{-\infty}^{\infty}\frac{d\tilde{\omega}}{2\pi}\int\frac{d^2k_\parallel}{(2\pi)^2}\frac{\mathrm{Im}\gamma(0)\mathrm{Im}\tilde{\gamma}(0)}{|\gamma(0)+\tilde{\gamma}(0)|^2}[n_F(\tilde{\omega}-\mu_L)-n_F(\tilde{\omega}-\mu_R)], \tag{26}$$

where $\tilde{\omega}=\omega_R+\mu_R=\omega_L+\mu_L$. For $T=0$ this can be recast into

$$\langle I(V)\rangle=8e\nu^{(2)}\int_{-\infty}^{\infty}\frac{d\tilde{\omega}}{2\pi}\int\frac{d^2k_\parallel}{(2\pi)^2}\frac{\mathrm{Im}\gamma(0)\mathrm{Im}\tilde{\gamma}(0)}{|\gamma(0)+\tilde{\gamma}(0)|^2}[\theta(\mu_L-\tilde{\omega})\theta(\tilde{\omega}-\mu_R)-\theta(\mu_R-\tilde{\omega})\theta(\tilde{\omega}-\mu_L)]. \tag{27}$$

In the limit $\mu_L\to\mu_R\to\mu$ (27) goes to

$$\langle I(V)\rangle=8e\nu^{(2)}\int_{\mu}^{\mu+eV}\frac{d\omega}{2\pi}\int\frac{d^2k_\parallel}{(2\pi)^2}\frac{\mathrm{Im}\gamma(0)\mathrm{Im}\tilde{\gamma}(0)}{|\gamma(0)+\tilde{\gamma}(0)|^2} \tag{28}$$

(see the discussion in Ref. 5 for the derivation). In the above expressions the imaginary parts of γ still contain the $k_\parallel$ dependence, which is not indicated for simplicity. According to its definition above, γ on the right hand side will receive a correction through the Dyson equation for g, yielding $\gamma=\gamma^0+\gamma'$, whereas for the left hand side there is no correction, so that $\tilde{\gamma}=\tilde{\gamma}^0$. Following CCNS it is assumed that for small bias $\gamma^0\simeq\tilde{\gamma}^0$ holds well. In order to get the first-order correction to the integrand in (28) it is expanded to first order in γ', yielding

$$\frac{\mathrm{Im}\gamma^0(\mathrm{Im}\gamma^0+\mathrm{Im}\gamma')}{|\gamma^0+(\gamma^0+\gamma')|^2}\simeq\frac{(\mathrm{Im}\gamma^0)^2}{|2\gamma^0|^2}+\frac{\mathrm{Im}\gamma^0\mathrm{Im}\gamma'}{|2\gamma^0|^2}+\frac{4(\mathrm{Im}\gamma^0)^2(\mathrm{Re}\gamma^0\mathrm{Re}\gamma'+\mathrm{Im}\gamma^0\mathrm{Im}\gamma')}{|2\gamma^0|^4}. \tag{29}$$

The expression for γ^0 is already given in Ref. 5 and can be written

$$\gamma^0=K\frac{iq\cosh Ka-K\sinh Ka}{K\cosh Ka-iq\sinh Ka}=\frac{-(q^2+K^2)\cosh Ka\sinh Ka+iqK}{K^2\cosh^2 Ka+q^2\sinh^2 Ka}K. \tag{30}$$

For arguments $Ka\sim4$ or larger, which seems reasonable for real tunneling processes, (30) goes asymptotically to the WKB-like result

$$\gamma^0\simeq-K+\frac{4iqK^2}{2mV_0}e^{-2Ka}. \tag{31}$$

This shows how the exponential dependence of the tunneling current on the barrier width enters this calculation.

The correction γ' is then obtained from the definition of γ by differentiating the correction term in the Dyson equation

$$\gamma'=-\frac{1}{2m}\lim_{x,x'\to0}\partial_x\partial_{x'}g^0(x,a)\Sigma(a,a)g^0(a,x')=-\frac{8mK^2}{D^2}\Sigma(a,a), \tag{32}$$

where again the dependence of g on $k_\parallel$ is not indicated explicitly. For reasons that will become apparent as we proceed, it is convenient to calculate the dimensionless ratios $\mathrm{Im}\gamma'/\mathrm{Im}\gamma^0$ and $\mathrm{Re}\gamma'/\mathrm{Re}\gamma^0$. Written in the following compact way we obtain

$$\left[\frac{\mathrm{Im}\gamma'}{\mathrm{Im}\gamma^0}\left|\frac{\mathrm{Re}\gamma'}{\mathrm{Re}\gamma^0}\right.\right]=\frac{8}{\pi}x_0^2V_0(2m)^{\frac{5}{2}}\left[V_0-\left(\omega+\mu-\frac{k_\parallel^2}{2m}\right)\right]\sqrt{\left(\mu-\frac{k_\parallel^2}{2m}\right)}\left[\frac{\mathrm{Im}\left(\frac{\Sigma^b}{D^2}\right)}{\mathrm{Im}\gamma^0}\left|\frac{\mathrm{Re}\left(\frac{\Sigma^b}{D^2}\right)}{\mathrm{Re}\gamma^0}\right.\right]. \tag{33}$$

Using the expressions introduced for γ^0 and D, (33) then yields

$$\left[\frac{\mathrm{Im}\gamma'}{\mathrm{Im}\gamma^0}\middle|\frac{\mathrm{Re}\gamma'}{\mathrm{Re}\gamma^0}\right]=C\left[\mathrm{Re}\Sigma^b+\mathrm{Im}\Sigma^b\frac{K^2-q^2}{2qK}\middle|2[2qK\mathrm{Im}\Sigma^b-(K^2-q^2)\mathrm{Re}\Sigma^b]\frac{e^{-2Ka}}{2mV_0}\right], \tag{34}$$

where $C=(8/\pi)mx_0^2\sqrt{(\mu-k_\parallel^2/2m)[V_0-(\omega+\mu-k_\parallel^2/2m)]}$. Equation (34) clearly shows that the second part of the square bracket is negligible for the small barrier transparencies considered here.

We can now conveniently write

$$\mathrm{Im}\gamma'=\mathrm{Im}\gamma^0\eta\ , \tag{35}$$

where we define $\eta=\mathrm{Im}\gamma'/\mathrm{Im}\gamma^0$. Inserting (35) into (29) now shows that the third term in (29) arising from the expansion of the denominator will be exponentially smaller than the first two, due to the exponential dependence of $\mathrm{Im}\gamma^0$. Thus (29) can be written

$$\frac{\mathrm{Im}\gamma^0(\,\mathrm{Im}\gamma^0+\mathrm{Im}\gamma')}{|\gamma^0+(\gamma^0+\gamma')|^2}\simeq\frac{(\mathrm{Im}\gamma^0)^2}{|2\gamma^0|^2}(1+\eta)\ .$$

So far all our results depend on $k_\parallel$, and as CCNS mention, the unperturbed expression in the integrand of (28) is a strongly peaked function around $k_\parallel=0$, which mainly comes from its exponential dependence on Ka. More precisely, differentiating with respect to V, (28) yields

$$\left\langle\frac{dI}{dV}\right\rangle=\int\frac{d^2k_\parallel}{(2\pi)^2}h\left(eV+\mu-\frac{k_\parallel^2}{2m}\right)\exp\left\{-4a\sqrt{2m\left[V_0-\left(eV+\mu-\frac{k_\parallel^2}{2m}\right)\right]}\right\}\ , \tag{36}$$

where h is a function that varies only slowly over the range of the integration compared to the exponential. Due to the strong exponential behavior of the final term, the largest contribution to this integration will come from the vicinity of the lower integration limit after transforming to polar coordinates. The square root in the exponential in (36) can be expanded in $z=k_\parallel^2$ around $k_\parallel=0$. The integrand can then be cast into

$$\begin{aligned}\left\langle\frac{dI}{dV}\right\rangle&=\int_0^\infty\frac{dz}{4\pi}h\left(eV+\mu-\frac{z}{2m}\right)\exp\{-4a\sqrt{2m[V_0-(eV+\mu)]}\}\exp\left\{\frac{-2az}{\sqrt{2m[V_0-(eV+\mu)]}}\right\}\\&\simeq\frac{\sqrt{2m[V_0-(eV+\mu)]}}{8\pi a}h(eV+\mu)\exp\{-4a\sqrt{2m[V_0-(eV+\mu)]}\}\ ,\end{aligned} \tag{37}$$

where we have neglected the contribution coming from the upper limit.

B. Discussion of $I(V)$, dI/dV, and d^2I/dV^2

The current-voltage characteristic $I(V)$ can now be obtained by integrating (36). For two reasons this procedure is not very rewarding. First, the integral is difficult to perform as the exchange term is no longer a slowly varying function over the range of integration, and thus our previous approximation of replacing $\int_x^{x+\delta x}f(x')dx'$ by $f(x)\delta x$ is not accurate. Second, the interesting corrections to $I(V)$, which come from the exchange diagram, are already very small in dI/dV (as will be shown later), so that the integration leading to $I(V)$ will make them essentially undetectable. We will thus concentrate on the expressions for the first and second derivatives of $I(V)$. The first derivative dI/dV, i.e., the differential conductivity, is simply given by (37) and accordingly d^2I/dV^2 can be obtained by a further differentiation. We thus have

$$\frac{dI}{dV}=\frac{e^2\nu^{(2)}}{2\pi^2a}\sqrt{2m[V_0-(eV+\mu)]}\frac{(\mathrm{Im}\gamma^0)^2}{|2\gamma^0|^2}(1+\eta)\ ,$$

$$\frac{d^2I}{dV^2}=\frac{e^2\nu^{(2)}}{2\pi^2a}\frac{d}{dV}\left[\sqrt{2m[V_0-(eV+\mu)]}\frac{(\mathrm{Im}\gamma^0)^2}{|2\gamma^0|^2}(1+\eta)\right]. \tag{38}$$

As an approximation to $(\mathrm{Im}\gamma^0)^2/|2\gamma^0|^2$ we have, consistent with our approximation in (36), taken over the WKB-expression (for $k_\parallel=0$) derived in Eq. (47) of Ref. 5 for further calculations,

$$\begin{aligned}\frac{(\mathrm{Im}\gamma^0)^2}{|2\gamma^0|^2}&=4\frac{(eV+\mu)[V_0-(eV+\mu)]}{V_0^2}\\&\quad\times\exp\{-4a\sqrt{2m[V_0-(eV+\mu)]}\}\ .\end{aligned} \tag{39}$$

We have used the expressions derived above to calculate the magnitude of these effects on the I-V characteristics of a model system, consisting of a single-crystal Si beam, rigidly clamped at both ends. The beam is chosen to have a length of 500 Å and a cross section of 100 Å × 100 Å, giving it a fundamental resonance frequency of $\omega_c/2\pi=30$ GHz and a mass of 1.2×10^{-20} kg. The effective spring constant of the beam will be 420 N/m. The parameters for the calculation are listed in Table I.

TABLE I. Parameters chosen for the model system. In the first row V_0 is the height of the barrier, μ the Fermi energy, and a the half barrier width. In the second row ω_c is the resonance frequency, m_c the mass, k_c the force constant, and Q the quality factor of the cantilever.

Barrier	$V_0=5$ eV	$\mu=2$ eV	$a=5$ Å	
Cantilever	$\omega_c=1.2\times10^{-4}$ eV	$m_c=1.2\times10^{-20}$ kg	$k_c=420$ N/m	$Q=10^3$

It should be noted that these results are calculated at $T=0$, and that a rather modest quality factor of 10^3 for the oscillator has been chosen. Mechanical oscillators at much lower ω_c, but with Q's of order 10^6 or higher have been reported.[13] Our choice of small Q was made to very roughly compensate for the finite temperature broadening effects in any actual experiment. As described in the Appendix, a Q of 10^3 corresponds roughly to a measurement on this system at 1 mK, but with a mechanical Q possibly much higher than 10^3.

Figures 5 and 6 show the first and second derivatives of the current density j (in A/m^2). The unperturbed terms for dI/dV and d^2I/dV^2 are not symmetric about the origin, since in our model we have assumed that the Fermi energy is fixed on one side of the barrier, while it is varied about this value by the bias on the other side. It can be seen that the relative magnitude of the exchange contribution in dI/dV to the unperturbed value is about 10^{-7} if temperature effects are neglected entirely. The form of the exchange part is similar to that observed for localized phonons. Comparing these graphs, it is apparent that it would be difficult to see the contribution of the exchange resonance after a final integration to get $I(V)$. The most visible feature is the correction to d^2I/dV^2: The exchange correction here reaches a size comparable to the unperturbed value, and the resonant form clearly distinguishes it from the smooth background.

Since the graphs only give a qualitative impression of the peak strengths, we now investigate them more thoroughly. The peaks in dI/dV clearly result only from contributions of the real part of the exchange term; cf. Eq. (25). The term has poles at $\omega=\pm b=\pm\omega_c\sqrt{1-(1/4Q^2)}$, which, in the bare term, leads to a peak height of $\mathrm{Re}\Sigma^b(\pm b)=\mp\frac{1}{2}[\ln 16+\ln Q^2]$, independent of ω_c. The origin of the peaks in d^2I/dV^2 is slightly more delicate. Here, the largest contributions come from the terms including $d/d\omega[\mathrm{Re}\Sigma^b(\omega)]$ and also $d/d\omega[\mathrm{Im}\Sigma^b(\omega)]$. The first term has poles at

$$\omega=\pm\sqrt{b^2+c^2\pm2c\sqrt{b^2+c^2}}$$
$$=\pm\omega_c\sqrt{1\pm\frac{1}{Q}}\simeq\pm\omega_c\left(1\pm\frac{1}{2Q}\right),$$

where the choices of the signs are made independently. The peak heights scale as $\pm Q/\omega_c$ for the outer (inner) poles, respectively. The second term has its poles exactly at $\omega=\pm b$, with heights that scale as $\pm 2Q/\omega_c$, and width [full width at half maximum (FWHM)] of ω_c/Q, and thus the peaks in the second derivative do depend on ω_c. To see how Q quantitatively affects the peak heights, we have compiled Table II of absolute heights of the maxima of the peaks in the exchange corrections to dI/dV and d^2I/dV^2, where apart from Q all other parameters for the system remain unchanged.

Eventually, as the intrinsic Q of the oscillator is increased, the broadening at zero temperature will be determined by electronic damping of the oscillator, given by higher-order terms in the self-energy. However, for the values of Q in the table, we believe these effects are unimportant.

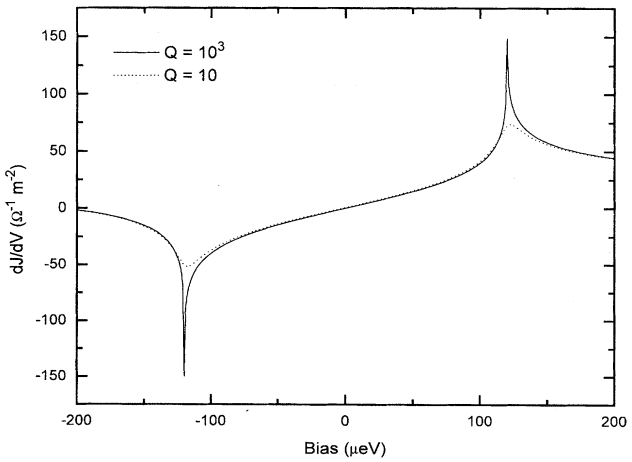

FIG. 5. Correction to the first derivative dJ/dV of the current density: the solid and dashed lines are for cantilever quality factors $Q=10^3$ and 10, respectively.

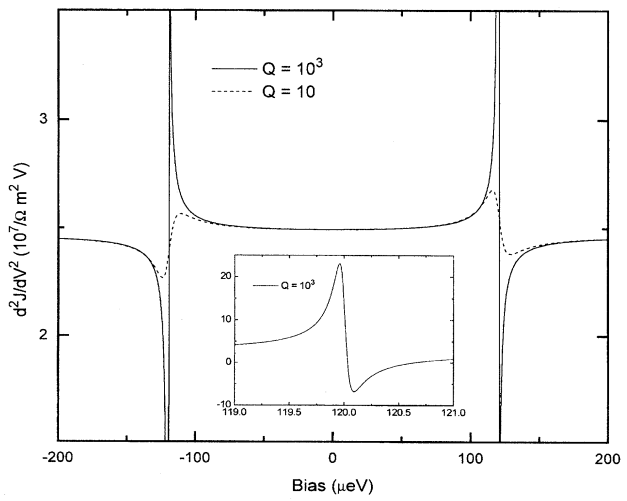

FIG. 6. Second derivative d^2J/dV^2 of the current density containing the corrections considered in the text; the solid and dashed lines are for $Q=10^3$ and 10, respectively. Inset: second derivative for $Q=10^3$, with vertical scale sufficient to show full extent of peaks. (Axes have same units as main plot.)

TABLE II. Calculated maxima of the peaks in the first and second derivatives of the tunneling current density over a range of values for the cantilever quality factor Q.

Q	10^3	10^4	10^5	10^6
dj/dV $[\Omega^{-1}\ \mathrm{m}^{-2}]$	150	188	227	265
d^2j/dV^2 $[G(\Omega V)^{-1}\ \mathrm{m}^{-2}]$	0.23	2.1	21	210

V. CONCLUSION

In conclusion we have investigated the first and most relevant self-energy corrections to the first and second derivatives of the $I(V)$ characteristic in M-I-M tunneling due to the interaction with a single localized mechanical mode of a movable tunnel junction. This represents the first step in investigating the influence of, and back action on, oscillatory mechanical degrees of freedom in a mesoscopic tunneling system. We find that the presence of this mechanical mode gives a pronounced signature in dI/dV, and a much stronger one in d^2I/dV^2, in the regions where the bias across the junction equals the energy of the eigenmode of the oscillator. This strong nonlinear enhancement of the differential conductivity and its derivative across the junction in this region can be viewed as arising from the opening of a new phonon-assisted channel for inelastic tunneling.

As the derivation of these results has been made using the general many-body formalism of CCNS, the approach may be readily extended. Possible applications might include considering stronger bias to generate a fully nonequilibrium situation, incorporating the band structure in the metals, and elucidating the role of other many-body interactions.

ACKNOWLEDGMENTS

We gratefully acknowledge helpful discussions with Professor Sir Roger J. Elliott at Oxford regarding theoretical specialties of this work. N.F.S. gratefully acknowledges financial support from Wolfson College, the Department of Theoretical Physics, and the Board of Graduate Studies of the University of Oxford. Furthermore, he would like to thank Ah San Wong for her kind support in organizing the end phase of this project.

APPENDIX

In this appendix we derive the range of validity of the zero temperature calculation and establish qualitatively the changes to our results as finite temperature effects start to compete with and finally dominate the intrinsic losses of the mechanical oscillator. The first zero temperature approximation which entered our calculation from before was in (18) for the Matsubara self-energy:

$$\Sigma^{1\mathrm{ex}}(i\omega_n)=-(x_0V_0)^2\sum_{k_x} f(k_x)\left[\frac{n_B(\omega_c)+n_F(\varepsilon_{\vec{k}})}{i\omega_n+\omega_c-\varepsilon_{\vec{k}}}+\frac{n_B(\omega_c)+1-n_F(\varepsilon_{\vec{k}})}{i\omega_n-\omega_c-\varepsilon_{\vec{k}}}\right]. \tag{A1}$$

If one still assumes that the largest contributions to the k_x sum come from the vicinity of the Fermi surface, one can approximate the sum similar to (22) as

$$\Sigma_r^{1\mathrm{ex}}(\omega)=-(x_0V_0)^2N^{1D}(0)f(\sqrt{2m\mu-k_\parallel^2})\times\left(n_B(\omega_c)\int_{-\infty}^{\infty}d\varepsilon\left[\frac{1}{\omega+\omega_c-\varepsilon+i\delta}+\frac{1}{\omega-\omega_c-\varepsilon+i\delta}\right]+\int_{-\infty}^{\infty}d\varepsilon\left[\frac{n_F(\varepsilon)}{\omega+\omega_c-\varepsilon+i\delta}+\frac{1-n_F(\varepsilon)}{\omega-\omega_c-\varepsilon+i\delta}\right]\right). \tag{A2}$$

The two integrals can be considered separately and the first one gives

$$\int_{-\infty}^{\infty}d\varepsilon\left[\frac{1}{\omega+\omega_c-\varepsilon+i\delta}+\frac{1}{\omega-\omega_c-\varepsilon+i\delta}\right]=\wp\int_{-\infty}^{\infty}d\varepsilon\frac{2(\omega-\varepsilon)}{(\omega-\varepsilon)^2-\omega_c^2}-2i\pi\,, \tag{A3}$$

where $\wp$ denotes the principle value. The principle value integral is seen to be zero, since the integral is antisymmetric. The imaginary part turns out to be constant with respect to ω. The second integral can be recast into

$$\int_{-\infty}^{\infty}d\varepsilon\left[\frac{n_F(\varepsilon)}{\omega+\omega_c-\varepsilon+i\delta}+\frac{1-n_F(\varepsilon)}{\omega-\omega_c-\varepsilon+i\delta}\right]=\wp\int_{-\infty}^{\infty}\frac{d\varepsilon}{e^{-\beta\varepsilon}+1}\,\frac{2\omega}{\omega^2-(\omega_c+\varepsilon)^2}-i\pi\int_{-\infty}^{\infty}d\varepsilon\frac{\delta(\varepsilon+\omega+\omega_c)+\delta(\varepsilon-\omega+\omega_c)}{e^{-\beta\varepsilon}+1}\,. \tag{A4}$$

If that is compared to formula (25), one sees that the difference for finite T is that the integrals now get a smooth cutoff at $\varepsilon=0$ as opposed to the θ-function cutoff from before. On introducing a finite quality factor Q, (A4) goes over to

$$\int_{-\infty}^{\infty}\frac{d\varepsilon}{e^{-\beta\varepsilon}+1}\left[\frac{(\omega+b+\varepsilon)-ic}{(\omega+b+\varepsilon)^2+c^2}+\frac{(\omega-b-\varepsilon)-ic}{(\omega-b-\varepsilon)^2+c^2}\right] \tag{A5}$$

in analogy to (25). We can thus choose either (A4) or (A5) as a basis of reasoning, depending on the regime considered. As it turns out, for the conceivable range of oscillator quality factors Q, the linewidths induced by Q will be very small compared to the temperature broadening, even for temperatures as small as ~ 1 mK. Thus, we assume for now that $Q\rightarrow\infty$ and use formula (A4). The difference in the behavior for the real part of (A4) above from its $T=0$ analog can be seen through partial integration:

$$\wp\int_{-\infty}^{\infty}\frac{1}{e^{-\beta\varepsilon}+1}\frac{2\omega}{\omega^2-(\omega_c+\varepsilon)^2}$$

$$=-\frac{\beta}{4}\int_{-\infty}^{\infty}\frac{d\varepsilon}{\cosh^2\frac{\beta}{2}\varepsilon}\ln\left|\frac{\omega-\omega_c-\varepsilon}{\omega+\omega_c+\varepsilon}\right| , \tag{A6}$$

where the integrated term has vanished at the boundaries. In the limit $\beta\rightarrow+\infty$

$$\frac{\beta}{4}\frac{1}{\cosh^2\frac{\beta}{2}\varepsilon}\rightarrow\delta(\varepsilon) . \tag{A7}$$

This way one can see how the $T=0$ result for the real part of (25) is recovered. The corresponding integration of the imaginary part gives

$$-i\pi\left[\frac{1}{e^{\beta(\omega+\omega_c)}+1}+\frac{1}{e^{-\beta(\omega-\omega_c)}+1}\right] , \tag{A8}$$

which for $\beta\omega_c\gg 1$ is seen to have a smoothed out step behavior, being essentially constant for $|\omega|>\omega_c+\delta_F$ and close to zero for $|\omega|<\omega_c-\delta_F$, where δ_F is the width (FWHM) of the Fermi distribution

$$\delta_F\simeq 3.5k_BT\simeq 3\times10^{-4}T \ \text{eV/K} . \tag{A9}$$

If (A8) is compared with the corresponding expression for $\mathrm{Im}\Sigma^b(\omega)$ in (25) at zero temperature but finite Q, the only difference is that in the present case δ_F rather than Q determines the deviation from a true step behavior, which is eventually attained as $T\rightarrow 0$ and $Q\rightarrow\infty$. From this it is possible to determine phenomenologically what effect temperature will have for the most "observable" of the peaks, i.e., the ones in d^2I/dV^2. The peaks in that function are, as we found, determined by $d\Sigma_r^{\mathrm{1ex}}(\omega)/d\omega$. It can be seen directly from (A8) that the derivative of the imaginary part, which gives the strongest contributions to these features, exhibits a pair of Lorentzian peaks at the resonance frequency of $\pm\omega_c$. At nonzero temperature these have a width determined by the Fermi distribution, as shown in (A9). One can also see the change in the behavior of the derivative of the real part of Σ from (A6) without having to perform the integral. Differentiating with respect to ω gives

$$-\frac{\beta}{4}\int_{-\infty}^{\infty}\frac{d\varepsilon}{\cosh^2\frac{\beta}{2}\varepsilon}\frac{2(\omega_c+\varepsilon)}{\omega^2-(\omega_c+\varepsilon)^2} . \tag{A10}$$

This can be viewed as being a sum of two convolutions of opposite sign in ω between the derivative of the Fermi function $1-n_F$ and the two partial fractions of the second factor. The result of the convolution of these two peaked functions is to a good approximation again a peaked function, where the width of the resulting feature is the sum of the widths of the convoluted components. Since for the moment we assume that the width of our initial peaks (due to the quality factor Q) is practically negligible compared to the thermal width of the Fermi function, the effective width of the peaks will also be given by the thermal width. If, on the other hand, in an intermediate regime (low Q, low T) the two effects start to compete, one would have to use (A5) for a correct treatment. However, as mentioned above, the effect will just be that the widths will add to give the result.

The second $T=0$ approximation was introduced in (27) for the current. In analogy to the reasoning above, one can argue that if the Fermi factors are kept the smoothed out cutoff will lead to similar effects, which will enhance the total broadening by an additional factor of about 2. In summary, we can conclude that the contributions of the quality factor Q and the temperature T to the total linewidth will be about

$$\left[\frac{\delta\omega}{\omega_c}\right]_Q=\frac{1}{Q} \quad \text{and} \quad \left[\frac{\delta\omega}{\omega_c}\right]_T=6\times10^{-4}\frac{\mathrm{eV}}{\mathrm{K}}\frac{T}{\omega_c} ,$$

and the total width will be approximately the sum of these two contributions.

*Permanent address: Department of Theoretical Physics, University of Oxford, 1 Keble Road, Oxford OX1 3NP, UK.

[1] M. F. Bocko, K. A. Stephenson, and R. H. Koch, Phys. Rev. Lett. **61**, 726 (1988).
[2] B. Yurke and G. P. Kochanski, Phys. Rev. B **41**, 8184 (1990).
[3] C. Presilla, R. Onofrio, and M. F. Bocko, Phys. Rev. B **45**, 3735 (1992).
[4] C. Caroli, R. Combescot, P. Nozières, and D. Saint-James, J. Phys. C **4**, 916 (1971).
[5] C. Caroli, R. Combescot, P. Nozières, D. Lederer, and D. Saint-James, J. Phys. C **4**, 2598 (1971).
[6] C. Caroli, R. Combescot, P. Nozières, and D. Saint-James, J. Phys. C **5**, 21 (1972).
[7] L. V. Keldysh, Sov. Phys. JETP **20**, 1018 (1965).
[8] J. Bardeen, Phys. Rev. Lett. **6**, 57 (1960).
[9] R. Combescot and G. Schreder, J. Phys. C **6**, 1363 (1973); R. Combescot and G. Schreder, J. Phys. C **7**, 1318 (1973).
[10] A. B. Migdal, Sov. Phys. JETP **7**, 996 (1958).
[11] G. Rickayzen, *Green's Functions and Condensed Matter* (Academic, New York, 1980).
[12] D. J. Scalapino, in *Superconductivity*, edited by R. D. Parks (Dekker, New York, 1969).
[13] R. N. Kleiman, G. K. Kaminsky, J. D. Reppy, R. Pindak, and D. J. Bishop, Rev. Sci. Instrum. **56**, 2088 (1985).